Fall 2019

M1 MELANOPSIN GANGLION CELLS IN THE Mus musculus RETINA ARE SIMILAR IN SHAPE AND SIZE

Geoffrey K. Sarpong
University of Akron, gks7@zips.uakron.edu

Honors Thesis

Presented to

The Honors College at The University of Akron

In Partial Fulfillment

of the Requirements for the Degree

Bachelor of Science (Honors)

GEOFFREY SARPONG

August, 2019

Abstract

An M1 melanopsin retinal ganglion cell (mRGC) is a subtype of the five melanopsin ganglion cells. The M1-type mRGC is distributed on the dorsal retina of a mouse and has an extensively overlapping dendritic network in both the sublamina a (OFF) and sublamina b (ON) layers of the inner plexiform layer. In the dorsal retina, the M1-type mRGCs are distinct and asymmetric.

The aim of this study was to examine the morphological similarity (shape and size) of M1-type mRGCs. The study traced 20 neurons in the first four months of a glaucoma retina of a DBA mouse, made measurements of the particular 20 neurons, and measured statistical interdependence between the 20 neurons in the first four-month old glaucoma retina of the DBA mouse using contemporary morphological data mean (Xiao-Sha et al., 2019).

It determined the morphological similarities (soma size, total dendritic length, dendritic field size, dendritic field diameter, and the number of branch points) of the 20 neurons using 2-D morphology tracing in ImageJ, of z stacks of confocal images from a triple labeled immunohistochemically stained four-month old glaucoma retina of the DBA mouse. This research also analyzed the morphological shapes of the 20 neurons, in the first four-month old glaucoma retina of the DBA mouse, using blender edited 3D prints. The ImageJ traces of the 20 neurons in the first four-month old glaucoma retina of the DBA mouse having M1-type mRGCs ramified within the ganglion cell layer. In the dorsal retina, the M1-type mRGCs are distinct and distributed asymmetry. The 20 neurons in the first four-month old glaucoma retina of the DBA mouse had size and shape conventional to the

M1-type mRGCs. All the measured morphological data (soma size, total dendritic length, dendritic field size, dendritic field diameter, and the number of branch points) resulted in p-values (0.6124 for soma size, 0.6396 for total dendritic length, 0.0778 for dendritic field size, 0.2599 dendritic field diameter, 0.3175 for the number of branches) above the set significance level ($\alpha = 0.05$). The statistical graphs showed the similarity in size and shape of the morphological data (soma size, total dendritic length, dendritic field size, dendritic field diameter, and the number of branch points) across the 20 neurons of the first four-month old glaucoma retina of the DBA mouse.

The findings of this research brings additional support to the existing findings of the morphological similarities within specific mRGCs subtypes (Ecker et al., 2010; Berson, Castrucci & Provencio, 2010).

Introduction

Retinal ganglion cells are the sole output neurons of the retina and have been implicated in the processing and projecting information to the visual centers (superior collicullis, lateral geniculate nucleus, and pretectal nuclei) from the retina. Adult RGCs (numberable population of retinal postmitotic neurons) are located mainly within the innermost nucleated layer (INL) of the mature retina, and the somata of some RGCs trace from the ganglion cell layer (final output neuron that takes visual world information from the retinal interneurons, bipolar cells and amacrine cells) to the inner plexiform layer (IPL) (Guerin, Mckernan, O'Brien, & Cotter, 2002). Adult mice have a finite population of RGCs output neurons competent of autonomous phototransduction and true photoreception, which

function as photopigment melanopsin (Provencio *et al*., 2000; Wee *et al.,* 2002). Developmental cell death results in the small population RGCs output neurons of mature mammalian retina. Meanwhile the specificity of RGC formation stems from the postmitotic development of a pluripotent progenitor retinal cell (Mu and Klein, 2004).

About 1.5-2.5% of retinal ganglion cells in a mouse's retina are intrinsically photosensitive retinal ganglion cells (ipRGCs) which express photopigment melanopsin (Hattar, Takao, Berson, & Yau, 2002; Morin et al., 2003; Sollars et al., 2003), and photoreceptor adaptation like in rods and cones (Wong et al., 2005; Do and Yau, 2013). The mRGCs regulate non-image forming (NIF) functions that include pupillary light reflex and circadian rhythms (Sondereker, Onyak, Islam, Ross, & Renna, 2017). The ipRGCs of RGCs receive classical photoreceptor input and send out monosynaptic projections (retinohypothalamic tract (RHT)) to the subset of subcortical visual nuclei of the brain including the suprachiasmatic nucleus (SCN), olivary pretectal nucleus (OPN), and the intergeniculate leaflet (IGL) (Goz et al., 2008; Guler et al., 2008; Hannibal and Fahrenkrug 2004; Hatori et al., 2008; Hattar et al., 2006). Thus, ipRGCs provide the sole pathway that regulates NIF and evoke hormonal response to light (Baver et al., 2008; Dacey et al., 2005; Gooley et al., 2003; Hannibal et al., 2004; Hattar et al., 2006; Hattar et al., 2002; Morin et al., 2003; Viney et al., 2007). RGCs known to express intrinsic photosensitivity were first thought to come from a single morphological subtype (defined as M1 or Type 1 in rodents) projecting to hypothalamic suprachiasmatic nucleus and other targets (Baver et al., 2008; Berson Dunn, & Takao, 2002; Hattar et al., 2006; Hattar et al., 2002; Morin et al., 2003; Sollars et al., 2003; Viney et al., 2007). Today, these ipRGCs can be classified into five

subtypes, M1-M5 (Dacey et al., 2005; Schmidt et al., 2008). The M1-type mRGCs are collateral bearing cell (Joo et al., 2013) and differ from the other subtypes of melanopsin ganglion cells in certain characteristics that includes the soma size, dendritic field size, axonal projections, level of melanopsin expression, retinal stratification (Hatter et al., 2002; Berson et al., 2010; Ecker et al., 2010; Schmidt and Kofuji, 2011; Llanos, J., Sáez, D., Palma-Behnke, R., Núñez, A., & Jiménez-Estévez, G., 2012).

M1-type mRGCs appear visibly on the dorsal retina of a mouse and have an extensively overlapping dendritic network in both the sublamina a (OFF) and sublamina b (ON) layers of the inner plexiform layer. In the dorsal retina, the M1-type mRGCs are distinct and distribute asymmetry. The M1-type mRGCs mainly synapse non-image forming (NIF) brain target encompassing olivary pretectal nucleus to implicates pupillary light reflex and suprachiasmatic nucleus to regulate circadian photoentrainment (Hattar et al., 2002; Baver et al., 2008; Guler et al., 2008; Schmidt et al., 2011). M1 melanopsin ganglion cells' somas projects from both ganglionic cell layer (GCL) and displaced M1d to inner nuclear layer (INL).

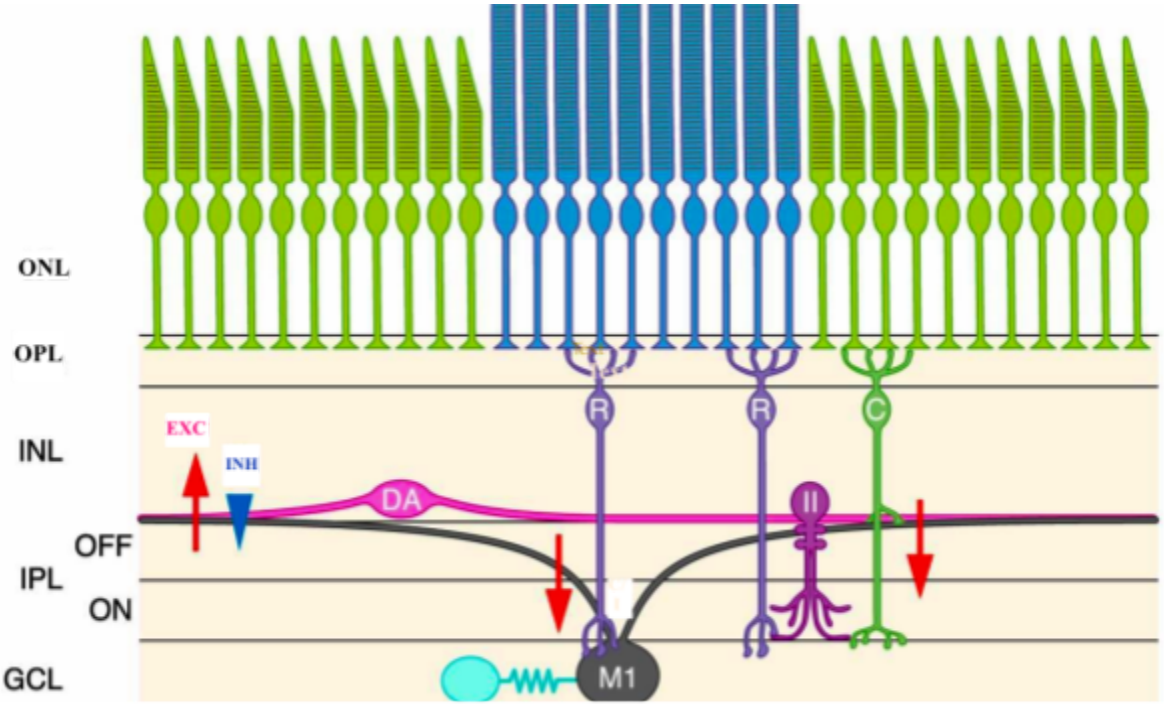

Figure 1

The outer nuclear layer (ONL), a photoreceptor layer, of the mouse retina contains rods and cones photoreceptors which innervates their respective rods (R) or cone bipolar cells in the outer plexiform layer (OPL). The inner nuclear layer (INL) regionalizes soma bipolar cells, amacrine (dopaminergic amacrine, DA; AII amacrine, II; and monostratified amacrine, MA) and horizontal (not identified in Figure 1) cells. The red arrow, blue arrow, upward-pointing arrow, and downward-pointing arrow demonstrate excitation, inhibition, signaling from ipRGCs, and signaling to ipRGCs respectively. Another dendritic-axonal interaction, the inner plexiform layer (IPL) delineates the inner nuclear layer from the ganglion cell layer.
Ganglion cell layer (GCL) contains ipRGCs coupled electrically to it, and also composed of retinal ganglion cells and melanopsin-positive class of retinal ganglion cells (not illustrated). The soma of the M1-type RGCs originated from the ganglion cell layer (GCL). Modified figure from (Do and Yau, 2010).

Existing findings report that M1-type mRGCs' constitute developmentally regulated dendritic network extends knowably to the biplexiform layer in the retina, but little is known about its morphology (similarity in shapes and sizes). As such, this research project provides a more complete description of M1-type mRGCs from morphological data (including soma size, total dendritic length, dendritic field size, dendritic field diameter and number of branch points).

Materials and Methods

Animals

All data in this study were obtained from the first four months old glaucoma retina of DBA mouse (Dr. Jordan's Lab) described previously by (Sondereker et al., 2017). All experiments were conducted in accordance with NIH procedures under protocols approved by the Institutional Animal Care and Use Committees of THE University of Akron. Animals were housed on a 12 hours dark cycle.

Visualization and quantification

Imaging of melanopsin immunopositive dendrites in wholemount retinas was done using an Olympus FV1000 software and an Olympus FV1000 confocal laser- scanning microscope with a 40x-oil or 60x-oil immersion objective. The confocal imaging containing z stacks were compiled at 0.45 to 1.0 micron intervals. ImageJ (NIH open access) was used to analyze the images, as well as adjust their contrast and brightness of the images with the

aid of Adobe Photoshop CS6.

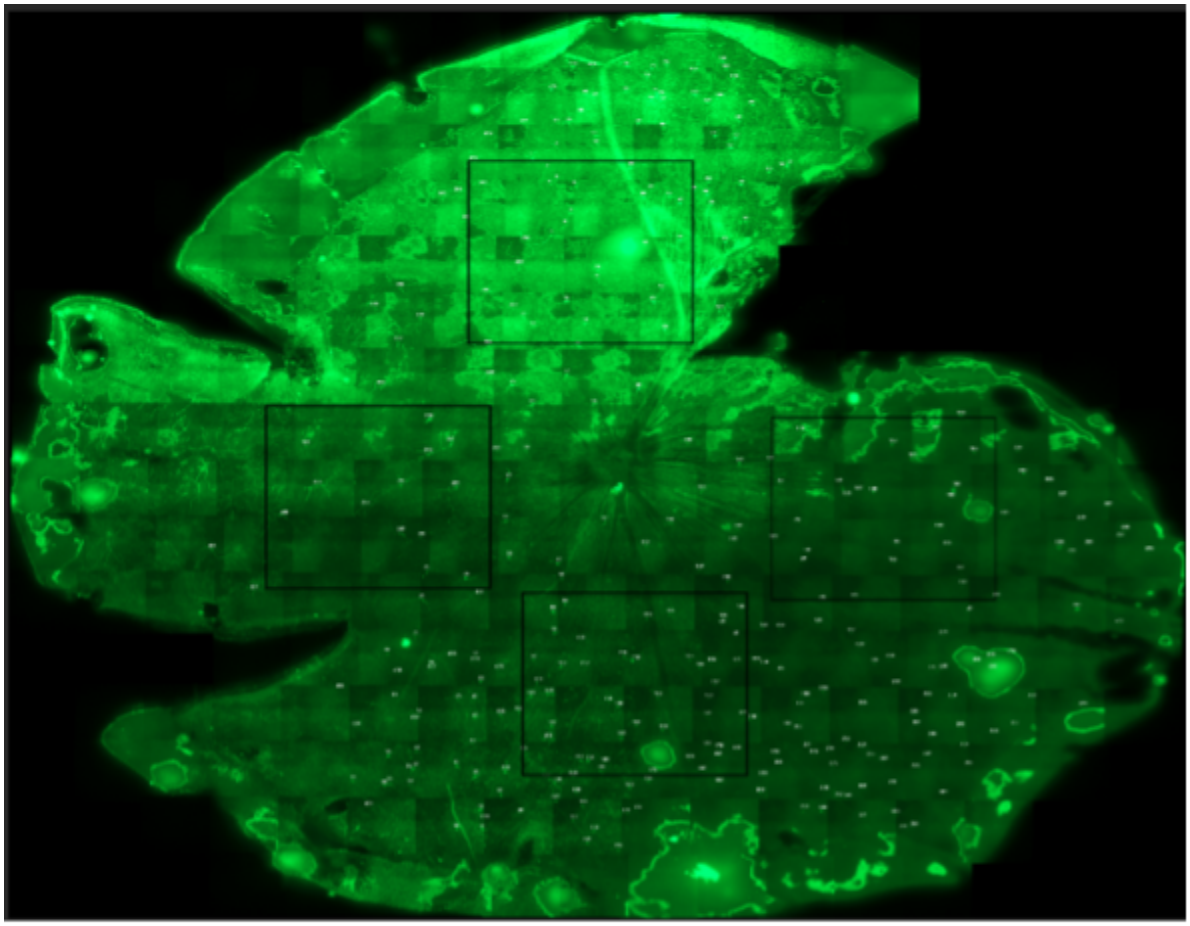

Figure 2

Image of the first four-month old glaucoma retina of the DBA mouse from adobe photoshop CS6. The tracings of M1-type mRGCs of the first four-month old glaucoma retina of the DBA mouse were from the upper squared area of the retina displaced in Figure 2.

Comparing the presence or absence of retinal cell bodies marked with DRAQ5 or DAPI identified the retinal stratification of melanopsin-positive dendrites regions. Outer plexiform layer (OPL) stratification was identified by VGLUT1 which was used as secondary marker (VGLUT1 marks photoreceptor terminals). Quantification involving the morphological data (soma size, total dendritic length, dendritic field size, dendritic field

diameter, and number of branch points) of M1-type mRGCs was done on M1-type mRGCs that stratify in the ganglion cell layer (GCL). ImageJ plugin, Simple Neurite Tracer measured the total dendritic length, dendritic field size, dendritic field diameter, and soma size (measurement taken from the longest distance across the cell bodies).

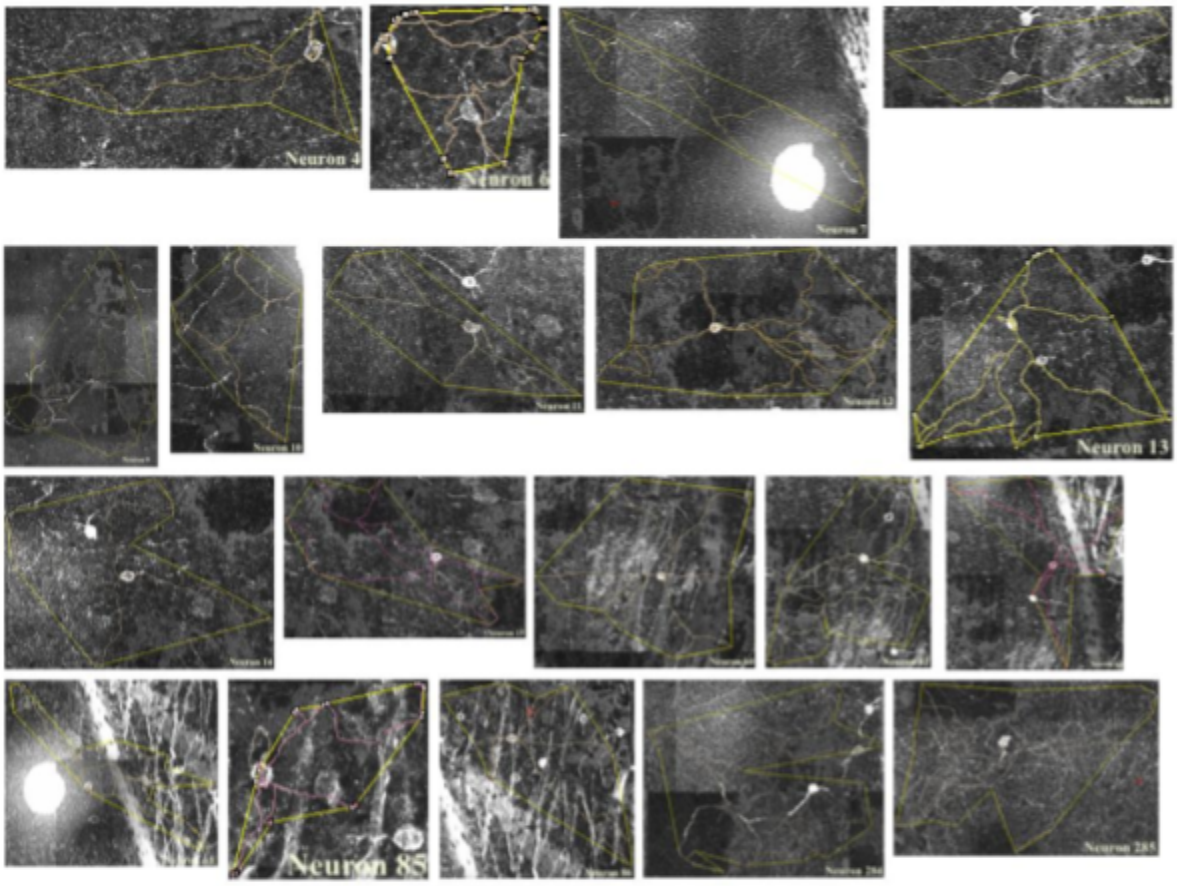

Figure 3
ImageJ tracings of 20M1-type mRGCs (neurons) in the first four-month old glaucoma retina of the DBA mouse.

The number of branch points was counted for each M1-type mRGCs using blender (free online software for the construction of 3D morphology of the neurons). The morphological values collected in ImageJ and from Blender were analyzed in StatCrunch (www.learn.uakron.edu/statcrunch5.0/).

Figure 4

Image of the 20 neurons in the first four-month old glaucoma retina of the DBA mouse edited using blender to construct 3D morphology.

Statistical Analysis

Statistical analysis was conducted to M1-type melanopsin retinal ganglion cells in the mouse retina are similar in shape and size using one sample Z hypothesis test, and chi-square test. Unless otherwise noted, data were valued as significant when $p > 0.05$ (with $\alpha = 0.05$), as determined using the one sample Z hypothesis test and chi-square test.

Results

The Morphological Data of the Soma Size (μm) from M1- type Melanopsin- Expressing Retinal Ganglion Cell

The somata in the ganglion cell layer (GCL) originating from M1-type mRGCs displayed an overall similarity in size as shown in the measurements below (Figure 5). The The similarity in somata size resulted in p- value of 0.6124 (Figure 5f) when compared with conventional soma size of M1-type mRGCs (Ecker et al., 2010) , and three graphs (Figure 5a-d) depicted graphical representation of the similarity in somata size gleaned from the morphological data. The recorded measurement summaries of the somata morphology are also illustrated below (Figure 5e-g).

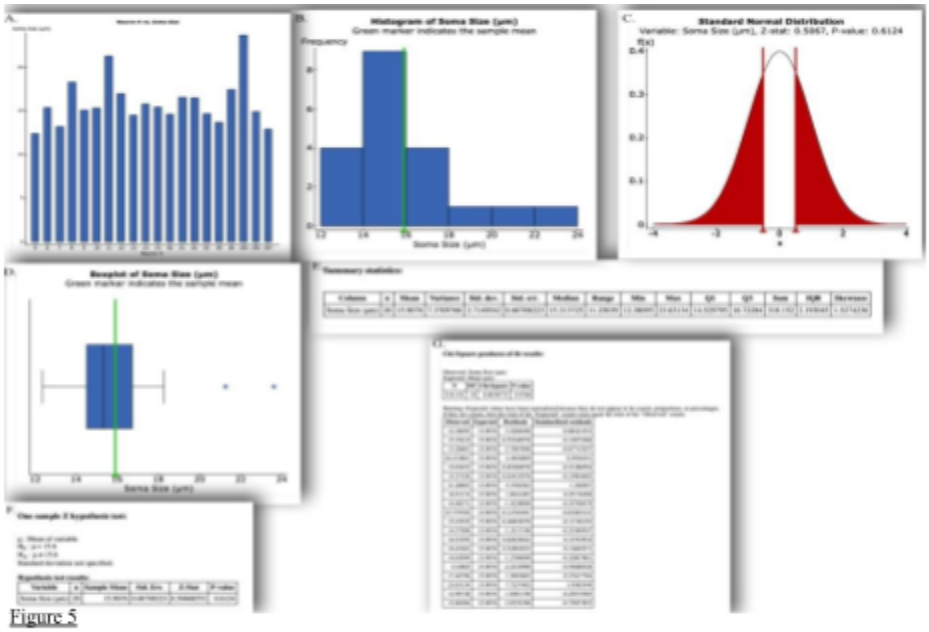

Figure 5

The Morphological Data of the Soma Size (µm) from M1- type Melanopsin- Expressing Retinal Ganglion Cell

a) Column chart depicts that the somata in the ganglion cell layer (GCL) originating from M1-type RGCs predominantly have soma size close to the mean and median. b) Histogram of the stomata in the ganglion cell layer (GCL) that originate from M1-type mRGCs confirms the clustering of the majority of the soma size towards the mean. c) Standard normal distribution of the stomata in the ganglion cell layer (GCL) that originate from M1-type RGCs illustrates disruptive bell-curve as a result of similarity in size of the sampled neurons ($p > 0.05$) close to conventional M1-type mRGCs. d) Box plot of the stomata in the ganglion cell layer (GCL) that originate from M1-type RGCs display two outliers in the soma size of the neurons. The soma size mean of the neurons were one place decimal from Ecker mean and Xiao-sha lesion mean . e) Summary statistics of the stomata in the ganglion cell layer (GCL) that originate from M1-type RGCs provides recorded measurement summary of the morphological data. f) One sample Z hypothesis test of the stomata in the ganglion cell layer (GCL) that originate from M1-type RGCs supports the hypothesis ("M1 MELANOPSIN GANGLION CELLS IN THE *Mus musculus* RETINA ARE SIMILAR IN SHAPE AND SIZE") generated for this thesis.g) Chi-square test of the stomata in the ganglion cell layer (GCL) that originate from M1-type RGCs shows 97.66% chance of finding similarity between the observed and expected (mean) distributions that is at least this extreme.

The Morphological Data of the Total Dendritic Length (µm) from M1- type Melanopsin- Expressing Retinal Ganglion Cell

The similarity in the entire length of the traced dendrites resulted in p- value of 0.6396 (Figure 6f). And statistical graphs were used to illustrate the similarities in the total dendritic length of the 20 neurons, that coincide with contemporary researchers' conventional M1-type RGCs total dendritic length (Xiao-Sha et al., 2019) . The overall average of the total dendritic length in the sublamina a (OFF) was 1064.4µm± 503.34µm (Figure 6a-f) . The recorded measurement summaries of the remaining morphological data were analyzed further with the chi-square test (Figure 6g).

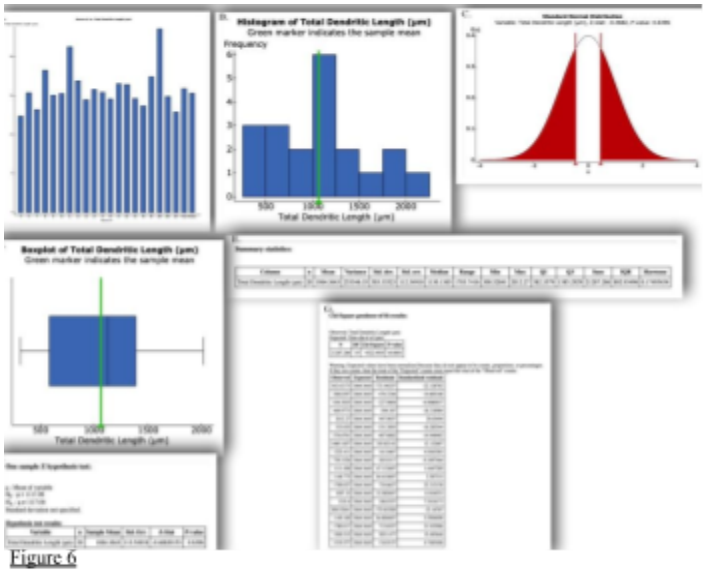

Figure 6

The Morphological Data of the Total Dendritic Length (µm) from M1- type Melanopsin- Expressing Retinal Ganglion Cell

a) Column chart depicts that the total dendritic length (µm) in the sublamina a (OFF) originating from M1-type RGCs predominantly have total dendritic length (µm) close to the mean and median. b) Histogram of the total dendritic length (µm) in the sublamina a (OFF) that originate from M1-type RGCs confirms the clustering of the majority of the soma size towards the mean. c) Standard normal distribution of the total dendritic in the sublamina a (OFF) that originate from M1-type RGCs illustrates disruptive bell-curve around contemporary researchers' conventional total dendritic length of M1-type RGCs as a result of similarity in size of the sampled neurons ($p > 0.05$). d) Box plot of the total dendritic length (µm)in the sublamina a (OFF) that originate from M1-type RGCs display higher third quartile in the total dendritic length (µm) of the neurons, and higher mean above contemporaries value. e) Summary statistics of the total dendritic length (µm) in the sublamina a (OFF) that originate from M1-type RGCs provides recorded measurement summary of the morphological data. f) One sample Z hypothesis test of the total dendritic length (µm) in the sublamina a (OFF) that originate from M1-type RGCs supports the hypothesis ("M1 MELANOPSIN GANGLION CELLS IN THE *Mus musculus* RETINA ARE SIMILAR IN SHAPE AND SIZE") generated for this thesis.g) Chi-square test of the total dendritic length (µm) in the sublamina a (OFF) that originate from M1-type RGCs displayed chi square analysis of the recorded morphological data .

The Morphological Data of the Dendritic Field Size (µm) from M1- type Melanopsin-Expressing Retinal Ganglion Cell

The morphological data of the areas of the retina where the dendrites cover resulted in p- value of 0.0778 (Figure 7f). Overall the dendritic field sizes from M1-type Melanopsin Expressing Retinal Ganglion Cells were close to the mean measurement of this research project and the mean value of contemporary researchers of the areas of the retina where the dendrites cover, and are well represented on the statistical graphs (Figure 7a-d). The morphological data of the areas of the retina where the dendrites cover had an outlier (Figure 7d), and few dendritic field size far from the mean (Figure 7a). Statistical summaries of the record morphological measurement are illustrated below (Figure 7e-g).

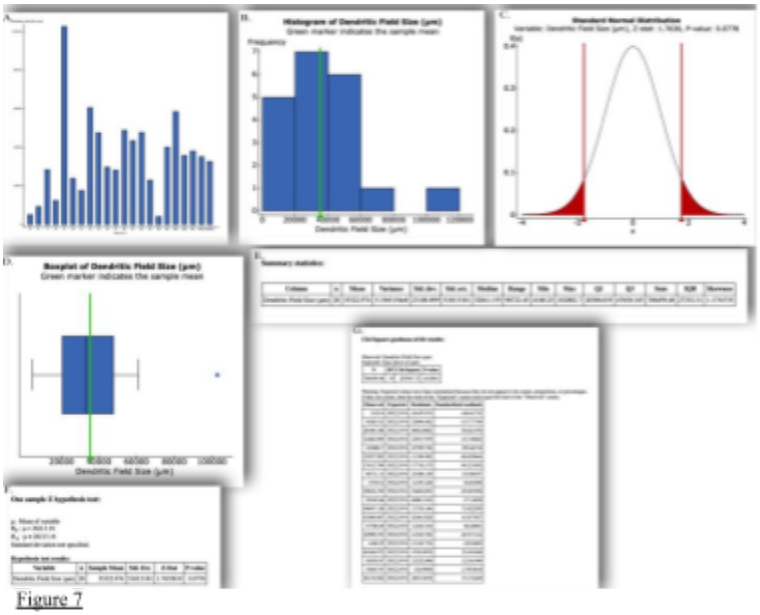

Figure 7

The Morphological Data of the Dendritic Field Size (µm) from M1- type Melanopsin- Expressing Retinal Ganglion Cell

a) Column chart depicts that the dendritic field size (µm) in the sublamina a (OFF) originating from M1-type RGCs predominantly have dendritic field size (µm) close to the mean and median. b) Histogram of the dendritic field size (µm) in the sublamina a (OFF) that originate from M1-type RGCs confirms the clustering of the majority of the size towards the mean. c) Standard normal distribution of the dendritic field size (µm) in the sublamina a (OFF) that originate from M1-type RGCs illustrates disruptive bell-curve around contemporary researchers' conventional values of the cells implying a similarity in size of the sampled neurons ($p > 0.05$). d) Box plot of the dendritic field size (µm) in the sublamina a (OFF) that originate from M1-type RGCs display an outlier in the dendritic field size (µm) of the neurons. e) Summary statistics of the dendritic field size (µm) in the sublamina a (OFF) that originate from M1-type RGCs provides recorded measurement summary of the morphological data. f) One sample Z hypothesis test of the dendritic field size (µm) in the sublamina a (OFF) that originate from M1-type RGCs supports the hypothesis ("M1 MELANOPSIN GANGLION CELLS IN THE *Mus musculus* RETINA ARE SIMILAR IN SHAPE AND SIZE") generated for this thesis.g) Chi-square test of the total dendritic in the sublamina a (OFF) that originate from M1-type RGCs displayed chi square analysis of the recorded morphological data .

The Morphological Data of the Dendritic Field Diameter (µm) from M1- type Melanopsin- Expressing Retinal Ganglion Cell

The morphological data dendritic field diameters from M1-type mRGCs were calculated from the area of the retina where the dendrites cover using the area of a circle equation ($A = \pi r^2$). The dendritic field diameters taken from the M1-type mRGCs resulted in p- value of 0.2599 (Figure 8f). The statistical graphical representation of the dendritic field diameters (Figure 8a-d) are similar to the statistical graphical representation of the dendritic field size) as both show the same magnitude of outlier. The statistical summaries of the dendritic field diameters are provided below (Figure 8e-g).

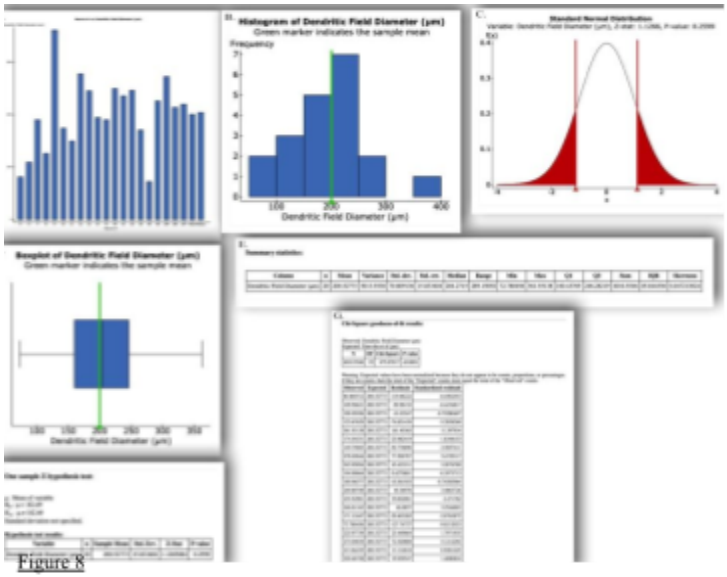

Figure 8

The Morphological Data of the Dendritic Field Diameter (μm) from M1- type Melanopsin- Expressing Retinal Ganglion Cell

a) Column chart depicts that the dendritic field diameter (μm) in the sublamina a (OFF) originating from M1-type RGCs predominantly have dendritic field diameter (μm) close to the mean and median. b) Histogram of the dendritic field diameter (μm) in the sublamina a (OFF) that originate from M1-type RGCs confirms the clustering of the majority of the size towards the mean. c) Standard normal distribution of the dendritic field diameter (μm) in the sublamina a (OFF) that originate from M1-type RGCs illustrates disruptive bell-curve around contemporary researchers' conventional values of the cells implying a similarity in size of the sampled neurons ($p > 0.05$). d) Box plot of the dendritic field diameter (μm) in the sublamina a (OFF) that originate from M1-type RGCs display higher third quartile in the dendritic field size (μm) of the neurons. e) Summary statistics of the dendritic field diameter (μm) in the sublamina a (OFF) that originate from M1-type RGCs provides recorded measurement summary of the morphological data. f) One sample Z hypothesis test of the dendritic field diameter (μm) in the sublamina a (OFF) that originate from M1-type RGCs supports the hypothesis ("M1 MELANOPSIN GANGLION CELLS IN THE *Mus musculus* RETINA ARE SIMILAR IN SHAPE AND SIZE") generated for this thesis.g) Chi-square test of the dendritic field diameter (μm) in the sublamina a (OFF) that originate from M1-type RGCs displayed chi square analysis of the recorded morphological data .

The Morphological Data of the Number of Branch Points from M1- type Melanopsin-Expressing Retinal Ganglion Cell

The morphological data of the number of branch points from M1-type mRGCs resulted in p- value of 0.3175 (Figure 9f). Statistical graphs represented the similarity in the number of branch points (Figure 9a-f, h) that conform with contemporary researchers' conventional M1-type RGCs number of branches (Xiao-Sha et al., 2019). Statistical summaries are represented below (Figure 9e-g).

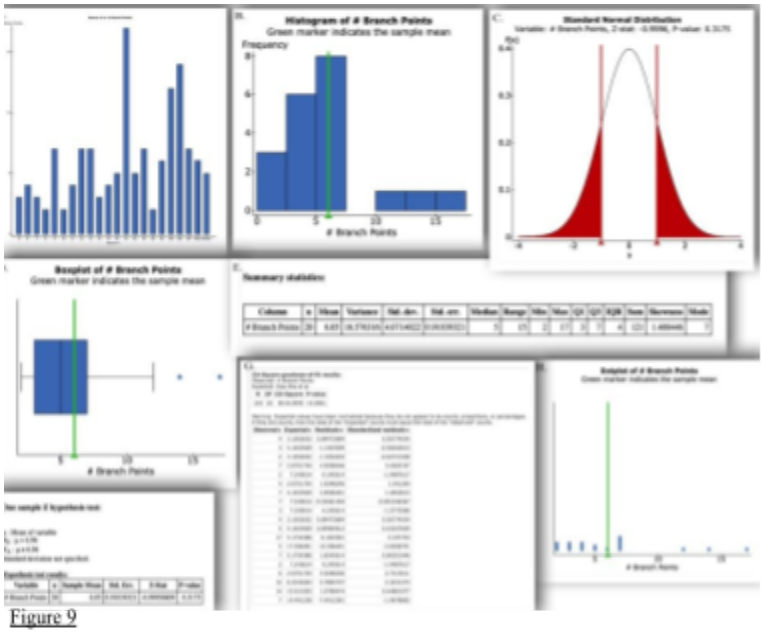

Figure 9

The Morphological Data of the Number of Branch Points from M1- type Melanopsin- Expressing Retinal Ganglion Cell

a) Column chart depicts that the number of branch points in the sublamina a (OFF) originating from M1-type RGCs predominantly have number of branch points close to the mean and median. b) Histogram of the number of branch points in the sublamina a (OFF) that originate from M1-type RGCs confirms the clustering of the majority of the number towards the mean. c) Standard normal distribution of the number of branch points in the sublamina a (OFF) that originate from M1-type RGCs illustrates disruptive bell-curve around contemporary researchers' conventional values of the cells implying a similarity in size of the sampled neurons ($p > 0.05$). d) Box plot of the number of branch points in the sublamina a (OFF) that originate from M1-type RGCs display higher third quartile in the number of branch points (µm) of the neurons, and higher contemporary mean to project mean value. e) Summary statistics of the number of branch points in the sublamina a (OFF) that originate from M1-type RGCs provides recorded measurement summary of the morphological data. f) One sample Z hypothesis test of the number of branch points in the sublamina a (OFF) that originate from M1-type RGCs supports the hypothesis ("M1 MELANOPSIN GANGLION CELLS IN THE *Mus musculus* RETINA ARE SIMILAR IN SHAPE AND SIZE") generated for this thesis.g) Chi-square test of the number of branch points

Discussion

The comparison within the M1-type mRGCs in the *Mus musculus* retina of having similar size and shape had good agreement. A statistical one sample Z hypothesis test was used to determine the similarities in morphological size within the M1-type mRGCs in the *Mus musculus* retina. The significance level for this project was set at 0.05. The five outcomes of the morphological data (soma size, total dendritic length, dendritic field size, dendritic field diameter, number of branch points) resulted in p- values (0.6124 for soma size, 0.6396 for total dendritic length, 0.0778 for dendritic field size, 0.2599 dendritic field

diameter, 0.3175 for the number of branches), which well all above 0.05 indicating that there were no significant differences and the data selection of the 20 neurons in the first four-month old glaucoma retina of the DBA mouse was random. A statistical Chi-Square goodness-to-fit was used to determine the similarities in morphological size within the M1-type mRGCs in the *Mus musculus* retina. The significance level was set at 0.05. The outcome of the soma size resulted in a p- value of .9766, which is above 0.05 indicating that there was no significant differences and the data selection of 20 neurons in the first four months old glaucoma retina of DBA mouse was random. The other chi-square test (in Figure 6g, 7g, 8g, and 9g) failed colossally to express significant similarities among the 20 neurons as a result of incomplete sampling data from the contemporary researchers on the topic of M1- type RGCs' morphological data A column chart, histogram, standard normal distribution, boxplot were simulated to analyze the similarities in morphological size within the M1-type mRGCs in the *Mus musculus* retina using contemporaries' conventional M1-type RGCs' morphological data. Dotplot was made to illustrate only the similarity in the number of branch points within the M1-type mRGCs, and to display the relatedness of sampled data to the contemporary's value. Results indicated there were colossal similarities in morphological size within the M1-type mRGCs in the *Mus musculus* retina as the morphological data always clouded around the contemporary mean morphological data. The graphs illustrated in Figure 5-9(a-d, 9h)were symmetrical showing that the five outcomes differed by an infinitesimal skewness values (Figure 5e, 6e, 7e, 8e, 9e) from the contemporary mean.

After discovering that the comparison of the size and shape within M1-type mRGCs in *Mus musculus* had good agreement, the median within five morphological data (soma size, total dendritic length, dendritic field size, dendritic field diameter, and number of branch points) were recorded. The soma size median of 20 neurons (all M1-type mRGCs) in the first four-month old glaucoma retina of the DBA mouse was 15.313725 microns, which differ by 0.593875 microns from the 15.9076± 2.714954249 micron soma size mean (Figure 5e) and 0.286275 microns from the contemporary mean value 15.6 ± 0.46 microns of the 20 neurons (all M1-type mRGCs) in the first four months old glaucoma retina of DBA mouse. The total dendritic length median of the 20 neurons (all M1-type mRGCs) in the first four-month old glaucoma retina of the DBA mouse was 1130.1365 microns, which differ by 65.772 microns from the 1064.3643±503.3352255micron (Figure 6e) total dendritic length mean and 13.075 microns from the contemporary mean value 117.06±55.98 microns of the 20 neurons (all M1-type mRGCs) in the first four months old glaucoma retina of DBA mouse. The dendritic field size median of the 20 neurons (all M1-type mRGCs) in the first four-month old glaucoma retina of the DBA mouse was 32841.155 microns, which differ by 2481.819 microns from the 35322.974± 23100.89904 microns (Figure 7e) dendritic field size mean and 6627.995 microns from the contemporary mean value of 26213.16 ± 3.25 micron of the 20 neurons (all M1-type mRGCs) in the first four-month old glaucoma retina of the DBA mouse. The dendritic field diameter median of 20 neurons (all M1-type mRGCs) in the first four-month old glaucoma retina of the DBA mouse was 72.780456 microns, which differ by 127.747274 microns from the 200.52773±70.80913637 micron (Figure 8e) mean and 110.18 microns from the contemporary mean value of 182.69±3.25

microns of the 20 neurons (all M1-type mRGCs) in the first four-month old glaucoma retina of the DBA mouse. The number of branch points median of the 20 neurons (all M1-type mRGCs) in the first four-month old glaucoma retina of the DBA mouse was 5, which differ by 1.05 from the 6.05±4.07140219 (figure 9e) mean and 0.91 from the contemporary mean value of 6.96±0.21 microns of the 20 neurons (all M1-type mRGCs) in the first four-month old glaucoma retina of the DBA mouse. The overall insignificance differences between the mean and median of this project together with the contemporary mean value and project median show colossal similarities in morphological size within the M1-type mRGCs in the *Mus musculus* retina. The morphological data mean of contemporary research used as the standard mean to analyze the M1-type RGCs similarity in morphological data was significant as the contemporary M1-type RGCs were diseased.

Based on the constructed 3D morphology of the 20 neurons in the first four-month old glaucoma retina of the DBA mouse edited using blender, there were no significance differences in the shapes. All the shapes of the 20 neurons in the first four-month old glaucoma retina of the DBA mouse were multipolar with either fewer or more dendritic branches (Figure 4). The shape that the dendrites of the 20 neurons in the first four-month old glaucoma retina of the DBA mouse forms is insignificant in determining morphological shape of the neurons. Dendrites from certain shapes as a result of their environment (Bear et al., 2016). However, some neurons in Figure 4 can arguably be classified as anaxonic neuron as a result of immunohistochemistry and imaging problems.

Limitation

There were multiple limitations in this research study that included the tracing of 20 neurons from a single diseased retina. The ImageJ traces of the 20 neurons was challenging as the result of improper z stack images stitchings. Also the quality of the z-stack images were not good, there was so much noise on the images attributed to incomplete immunohistochemistry. The unavailability of conventional morphological data database of M1-type RGCs created a difficulty.

Conclusion

The morphological analysis of M1-type mRGCs is the first step in characterizing the importance of melanopsin-expressing retinal ganglion cell that broadly supports the existing findings of retinal ganglion cells. The goal of this research was to examine the morphology (shape and size) of M1-type mRGCs by tracing 20 M1-type mRGCs, and to determine whether M1-type mRGCs are similar in shape and size.The research findings brings additional support in favor of the conventional size and shape of M1-type mRGCs. Comparing morphological data (soma size, total dendritic length, dendritic field size, dendritic field diameter, and number of branch points) within the 20 neurons in the first four-month old glaucoma retina of the DBA mouse with contemporary morphological data showed similarity trend that exist among M1-type mRGCs. Statistical results and 3D construction of the neurons morphologies supported the morphological similarity in size and shape of M1-type mRGCs traced for this project and contemporary articles (including Xiao-Sha et al., 2019)..

This project included few data set because of neuron sampling, therefore the results should not be interpreted as an accurate findings of the conventional size and shape of M1-type mRGCs. However, the project provides potential research projects, guidelines, and ideas that could lead to improving future findings of the conventional size and shape of M1-type mRGCs. Future research should concentrate on sampling more neurons from different healthy retinas containing M1-type mRGCs, and analyze morphological data from the different healthy retinas containing M1-type mRGCs using two way ANOVA testing. The morphological data of the M1-type RGCs from numerous mouse retinas can be used to create large database.

Acknowledgements

"For I *am* the LORD, I change not; therefore ye sons of Jacob are not consumed, Malachi 3:6." I give ceaseless praise to the Almighty GOD who raised up My Father Apostle Johnson Suleman to wipe out my tears and restore destinies. I thank My Father Apostle Johnson Suleman and My Mother Lizzy Johnson Suleman for their constant prayers and innumerable instructions from the GOSPEL that have completely change my life for the best plan of GOD for my life. Thank you to Professor Jordan Renna for serving as the research sponsor, and providing magnomous support with this honors project. I would like to gratefully appreciate the help of Professor Jordan's research lab group, and well need of mention Mrs. Jessica Onyak, who confirmed all the data collected and served as an oversight with the honors project. I also would like to appreciate the kind gestures of

Professor Quin Liu and Professor Brian Bagatto, who served as the readers of this honors project.

References

Baver, S. B., Pickard, G. E., Sollars, P. J., & Pickard, G. E. (2008). Two types of melanopsin retinal ganglion cell differentially innervate the hypothalamic suprachiasmatic nucleus and the olivary pretectal nucleus. *European Journal of Neuroscience*, *27*(7), 1763-1770

Bear, M. F., Connors, B. W., & Paradiso, M. A. (2016). *Neuroscience: Exploring the brain*. Philadelphia [etc.: Wolters Kluwer

Bellocchio EE, Reimer RJ, Fremeau RT Jr, Edwards RH (2000) Uptake of glutamate into synaptic vesicles by an inorganic phosphate transporter. Science 289:957–960

Berson DM, Dunn FA, Takao M (2002) Phototransduction by retinal ganglion cells that set the circadian clock. Science 295:1070–1073

Dacey, D. M., Liao, H. W., Peterson, B. B., Robinson, F. R., Smith, V. C., Pokorny, J., ... & Gamlin, P. D. (2005). Melanopsin-expressing ganglion cells in primate retina signal colour and irradiance and project to the LGN. *Nature*, *433*(7027), 749

Do, M. T. H., & Yau, K. W. (2013). Adaptation to steady light by intrinsically photosensitive retinal ganglion cells. *Proceedings of the National Academy of Sciences*, *110*(18), 7470-7475

Do MT, Yau KW. Intrinsically photosensitive retinal ganglion cells. *Physiol Rev*. 2010;90(4):1547–1581. doi:10.1152/physrev.00013.2010

Gooley, J. J., Lu, J., Fischer, D., & Saper, C. B. (2003). A broad role for melanopsin in nonvisual photoreception. *Journal of Neuroscience*, *23*(18), 7093-7106

Göz, D., Studholme, K., Lappi, D. A., Rollag, M. D., Provencio, I., & Morin, L. P. (2008). Targeted destruction of photosensitive retinal ganglion cells with a saporin conjugate alters the effects of light on mouse circadian rhythms. *PloS one*, *3*(9), e3153

Guerin, M. B., Mckernan, D. P., O'Brien, C. J., & Cotter, T. G. (2002). Retinal ganglion cells: dying to survive. International Journal of Developmental Biology, 50(8), 665-674

Güler, A. D., Ecker, J. L., Lall, G. S., Haq, S., Altimus, C. M., Liao, H. W., ... & Hankins, M. W. (2008). Melanopsin cells are the principal conduits for rod–cone input to non-image-forming vision. *Nature*, *453*(7191), 102

Hannibal J, Fahrenkrug J (2004) Target areas innervated by PACAP- immunoreactive retinal ganglion cells. Cell Tissue Res 316:99–113

Hatori M, Le H, Vollmers C, Keding SR, Tanaka N, Buch T, Waisman A, Schmedt C, Jegla T, Panda S (2008) Inducible ablation of melanopsin-expressing

retinal ganglion cells reveals their central role in non-image forming visual responses. PLoS ONE 3:e2451

Hattar, S., Kumar, M., Park, A., Tong, P., Tung, J., Yau, K. W., & Berson, D. M. (2006). Central projections of melanopsin‐expressing retinal ganglion cells in the mouse. *Journal of Comparative Neurology*, *497*(3), 326-349

Hattar, S., Liao, H. W., Takao, M., Berson, D. M., & Yau, K. W. (2002). Melanopsin-containing retinal ganglion cells: Architecture, projec- tions, and intrinsic photosensitivity. Science, 295(5557), 1065–1070

Haverkamp, S., Grünert, U., & Wässle, H. (2001). The synaptic architecture of AMPA receptors at the cone pedicle of the primate retina. *Journal of Neuroscience*, *21*(7), 2488-2500

Hughes, S., Watson, T. S., Foster, R. G., Peirson, S. N., & Hankins, M. W. (2013). Nonuniform distribution and spectral tuning of photosensitive retinal ganglion cells of the mouse retina. Current Biology, 23(17), 1696-1701

Johnson, J., Tian, N., Caywood, M. S., Reimer, R. J., Edwards, R. H., & Copenhagen, D. R. (2003). Vesicular neurotransmitter transporter expression in developing postnatal rodent retina: GABA and glycine precede glutamate. *Journal of Neuroscience*, *23*(2), 518-529

Joo, H. R., Peterson, B. B., Dacey, D. M., Hattar, S., & Chen, S. K. (2013). Recurrent axon collaterals of intrinsically photosensitive retinal ganglion cells. *Visual neuroscience*, *30*(4), 175-182

Llanos, J., Sáez, D., Palma-Behnke, R., Núñez, A., & Jiménez-Estévez, G. (2012, June). Load profile generator and load forecasting for a renewable based microgrid using self organizing maps and neural networks. In *The 2012 International Joint Conference on Neural Networks (IJCNN)* (pp. 1-8). IEEE

Morin, L. P., Blanchard, J. H., & Provencio, I. (2003). Retinal ganglion cell projections to the hamster suprachiasmatic nucleus, intergeniculate leaflet, and visual midbrain: bifurcation and melanopsin immunoreactivity. *Journal of Comparative Neurology*, *465*(3), 401-416

MU, X. and KLEIN, W.H. (2004). A gene regulatory hierarchy for retinal ganglion cell specification and differentiation. Semin Cell Dev Biol 15: 115-23.

Panda S, Provencio I, Tu DC, Pires SS, Rollag MD, Castrucci AM, Pletcher MT, Sato TK, Wiltshire T, Andahazy M, Kay SA, Van Gelder RN, Hogenesch JB (2003) Melanopsin is required for non- image-forming photic responses in blind mice. Science 301:525–527

Phillips, M. J., Otteson, D. C., & Sherry, D. M. (2010). Progression of neuronal and synaptic remodeling in the rd10 mouse model of retini- tis pigmentosa. The Journal of Comparative Neurology, 518(11), 2071–2089

Popova, E. (2015). GABAergic neurotransmission and retinal ganglion cell function. Journal of Comparative Physiology A, 201(3), 261-283

Provencio, I., Rodriguez, I. R., Jiang, G., Hayes, W. P., Moreira, E. F., & Rollag, M. D. (2000). A novel human opsin in the inner retina. *Journal of Neuroscience*, *20*(2), 600-605

Pramanik, N., & Panda, R. K. (2009). Application of neural network and adaptive neuro-fuzzy inference systems for river flow prediction. *Hydrological Sciences Journal*, *54*(2), 247-260

Schiviz, A. N., Ruf, T., Kuebber‐Heiss, A., Schubert, C., & Ahnelt, P. K. (2008). Retinal cone topography of artiodactyl mammals: influence of body height and habitat. *Journal of Comparative Neurology*, *507*(3), 1336-1350

Schmidt, T. M., & Kofuji, P. (2011). Structure and function of bistratified intrinsically photosensitive retinal ganglion cells in the mouse. *Journal of Comparative Neurology*, *519*(8), 1492-1504

Schmidt, T. M., Taniguchi, K., & Kofuji, P. (2008). Intrinsic and extrinsic light responses in melanopsin-expressing ganglion cells during mouse development. *Journal of neurophysiology*, *100*(1), 371-384

Sekaran, S., Lupi, D., Jones, S. L., Sheely, C. J., Hattar, S., Yau, K. W., . . .Hankins, M. W. (2005). Melanopsin-dependent photoreception pro- vides earliest light detection in the mammalian retina. Current Biology: CB, 15(12), 1099–1107

Sherry, D. M., Wang, M. M., Bates, J., & Frishman, L. J. (2003). Expres- sion of vesicular glutamate transporter 1 in the mouse retina reveals temporal ordering in

development of rod vs. cone and ON vs. OFF circuits. The Journal of Comparative Neurology, 465(4), 480–498

Sollars, P. J., Smeraski, C. A., Kaufman, J. D., Ogilvie, M. D., Provencio, I., & Pickard, G. E. (2003). Melanopsin and non-melanopsin expressing retinal ganglion cells innervate the hypothalamic suprachiasmatic nucleus. *Visual neuroscience*, *20*(6), 601-610

Sondereker, K. B., Onyak, J. R., Islam, S. W., Ross, C. L., & Renna, J. M. (2017). Melanopsin ganglion cell outer retinal dendrites: Morphologically distinct and asymmetrically distributed in the mouse retina. Journal of Comparative Neurology, 525(17), 3653-3665

Wee, R., Castrucci, A. M., Provencio, I., Gan, L., & Van Gelder, R. N. (2002). Loss of photic entrainment and altered free-running circadian rhythms in math5−/− mice. *Journal of Neuroscience*, *22*(23), 10427-10433

Wong-Riley, M. T., Liang, H. L., Eells, J. T., Chance, B., Henry, M. M., Buchmann, E., ... & Whelan, H. T. (2005). Photobiomodulation directly benefits primary neurons functionally inactivated by toxins role of cytochrome c oxidase. *Journal of Biological Chemistry*, *280*(6), 4761-4771

Wu, X. S., Wang, Y. C., Liu, T. T., Wang, L., Sun, X. H., Wang, L. Q., ... & Zhong, Y. M. (2019). Morphological alterations of intrinsically photosensitive retinal ganglion cells after ablation of mouse photoreceptors with selective photocoagulation. *Experimental eye research*, *188*, 107812

Viney, T. J., Balint, K., Hillier, D., Siegert, S., Boldogkoi, Z., Enquist, L. W., ... & Roska, B. (2007). Local retinal circuits of melanopsin-containing ganglion cells identified by transsynaptic viral tracing. *Current Biology*, *17*(11), 981-988